

Molecular Structures of Titanium(IV) and Vanadium(IV) Amides and Alkoxides†

Arne Haaland,^{*a} Kristin Rypdal,^{*a} Hans Vidar Volden^a and Richard A. Andersen^b

^a Department of Chemistry, University of Oslo, Box 1033 Blindern, 0315 Oslo, Norway

^b Department of Chemistry, University of California, Berkeley, CA 94720, USA

Gas-phase electron diffraction data for $\text{Ti}(\text{NMe}_2)_4$, $\text{V}(\text{NMe}_2)_4$ and $\text{V}(\text{OBu}^t)_4$ obtained with nozzle temperatures of 130–156 °C are consistent with molecular models of S_4 symmetry. The metal to ligand bond distances (r_s) are Ti–N 191.7(3), V–N 187.9(4) and V–O 177.9(6) pm, respectively. A set of bonding radii for Ti^{IV} , V^{IV} , Cr^{IV} and W^{VI} for use with the modified Schomaker–Stevenson rule is proposed. The valence angle bisected by the S_4 axis in the titanium amide, N–Ti–N 114.2(17)°, indicates that the co-ordination tetrahedron is slightly flattened. The corresponding angles in the vanadium amide and alkoxide are N–V–N 100.6(5)° and O–V–O 115.1(19)°, indicating that the co-ordination polyhedron in the former is significantly elongated, while in the latter it is significantly flattened. The shapes of the co-ordination tetrahedra in these and related molecules are discussed in terms of donation of π electrons from N or O into low-lying d orbitals on the metal atom.

Relatively few studies have been made of a series of homoleptic molecules MX_n , where only one variable, the metal, the ligand or the oxidation number, is changed in a systematic manner. The present study is part of a project aimed at the structure determination of homoleptic transition-metal compounds MX_n , where M is a Group 4, 5 or 6 metal, the ligand X is an alkyl, dimethylamino or *tert*-butoxy group, and the co-ordination and oxidation numbers n are 4. An X-ray study of $\text{Mo}(\text{NMe}_2)_4$ ¹ and a gas-phase electron diffraction (GED) study of $\text{Zr}(\text{NMe}_2)_4$ ² have been published by others. We have previously investigated the GED structure of $\text{Cr}(\text{OBu}^t)_4$ ³ and the molecular structure of $\text{Cr}(\text{CH}_2\text{Me}_3)_4$ ⁴ has been published recently. We have, however, been unsuccessful in our attempts at recording GED data for $\text{Ti}(\text{CH}_2\text{SiMe}_3)_4$, $\text{Ti}(\text{OBu}^t)_4$ and $\text{Zr}(\text{CH}_2\text{CMe}_3)_4$.

In this paper we report the gas-phase thermal average molecular structures of $\text{Ti}(\text{NMe}_2)_4$, $\text{V}(\text{NMe}_2)_4$ and $\text{V}(\text{OBu}^t)_4$. In our discussion of the structures determined to date we emphasize metal–ligand bond distances as well as deviation from perfect tetrahedral co-ordination geometry about the metal atom. Both the amides and the alkoxide have been investigated by various spectroscopic methods (IR, NMR, PS and ESR).^{5–7} These studies provided some evidence for distortion of the MN_4 or MO_4 skeletons, particularly when $\text{M} = \text{V}$.

Experimental

Syntheses.— $\text{V}(\text{OBu}^t)_4$. Vanadium tetra-*tert*-butoxide was prepared by a synthetic method analogous to that used to prepare $\text{Cr}(\text{OBu}^t)_4$.⁸ Solid $\text{VCl}_3(\text{thf})_3$ ($\text{thf} = \text{tetrahydrofuran}$) (16.7 g, 0.035 mol) was added slowly over 24 h to LiOBu^t (11.3 g, 0.14 mol) in hexane (125 cm³) and thf (50 cm³). Solid CuCl (3.5 g, 0.035 mol) was added to the blue-purple suspension and the mixture was refluxed for 3 h. The blue suspension was allowed to cool to room temperature, settle and filtered. The filtrate was evaporated to dryness and the blue oil was distilled at 85–90 °C at 0.1 mmHg (lit.⁹ 60–70 °C at 0.1 mmHg) giving 8.3 g (63% yield) of $\text{V}(\text{OBu}^t)_4$. UV (pentane): 720 and 850(sh) nm [lit.:⁷ 719 and 914(sh) nm (benzene)].

$\text{V}(\text{NMe}_2)_4$. Vanadyl chloride, VOCl_3 (4.15 g, 0.024 mol), was added dropwise to LiNMe_2 (6.3 g, 0.12 mol) suspended in pentane (120 cm³) at 0 °C. The green suspension was warmed to

Table 1 Nozzle temperatures, number of exposed plates and s limits for GED intensity curves of $\text{Ti}(\text{NMe}_2)_4$, $\text{V}(\text{NMe}_2)_4$ and $\text{V}(\text{OBu}^t)_4$

	$\text{Ti}(\text{NMe}_2)_4$	$\text{V}(\text{NMe}_2)_4$	$\text{V}(\text{OBu}^t)_4$
Nozzle temperature/ °C	152–155	130–155	152–156
Number of plates			
50 cm	5	5	6
25 cm	5	10	4
s limits/nm ⁻¹			
50 cm	25.00–148.75	20.00–135.00	30.00–148.75
($\Delta s = 1.25 \text{ nm}^{-1}$)			
25 cm	25.00–280.00	40.00–265.00	70.00–245.00
($\Delta s = 2.50 \text{ nm}^{-1}$)			

room temperature and stirred for 12 h. It was then filtered and the filtrate evaporated to dryness. The green semi-solid residue was distilled at 50–60 °C at 10⁻² mmHg to give 2.0 g (37% yield) of green, solid $\text{V}(\text{NMe}_2)_4$. UV (pentane) 559 and 750 nm [lit.:⁷ 559 and 752 nm (benzene)].

The compound $\text{Ti}(\text{NMe}_2)_4$ was prepared as described by Andersen *et al.*¹⁰

Gas-phase Electron Diffraction.—Data were recorded on a Balzers Eldigraph KDG-2 instrument.^{11,12} Two data sets were recorded for each molecule, with nozzle-to-plate distances of 50 and 25 cm, respectively. After photometry of the photographic plates the data were processed by standard procedures.¹³ Backgrounds were computer drawn and an average curve was calculated for each data set. Atomic scattering factors were taken from ref. 14. Information about the experiment (nozzle temperature, number of exposed plates) and s limits in the final refinements is given in Table 1. Intensity curves for $\text{V}(\text{NMe}_2)_4$ and $\text{V}(\text{OBu}^t)_4$ are shown in Figs. 1 and 2, respectively; those of $\text{Ti}(\text{NMe}_2)_4$ cannot be visually distinguished from the ones of the vanadium analogue.

Model Choice and Refinements.— $\text{M}(\text{NMe}_2)_4$ ($\text{M} = \text{Ti}$ or V). Structure refinements were based on models with overall S_4 symmetry, NCH_3 fragments of C_{3v} symmetry and $\text{MN}(\text{CH}_3)_2$ fragments of C_2 symmetry. The latter assumption implies that the co-ordination sphere around the N atoms is planar as found in previous studies of $\text{Mo}(\text{NMe}_2)_4$ and $\text{Zr}(\text{NMe}_2)_4$.^{1,2}

† Non-SI unit employed: mmHg \approx 133 Pa.

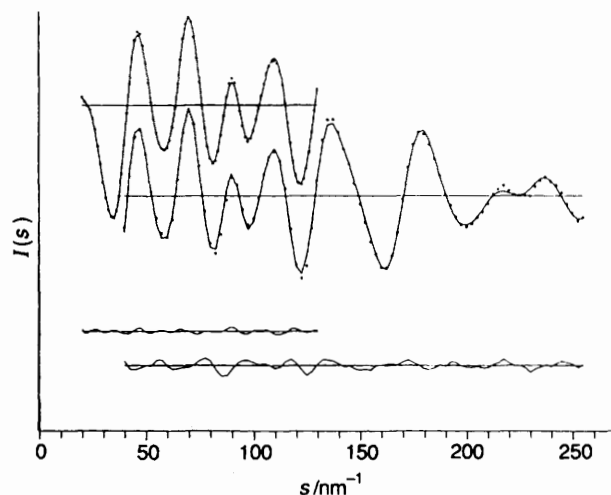


Fig. 1 Calculated (full line) and experimental (●) intensity curves for $\text{Ti}(\text{NMe}_2)_4$ with the difference curves shown below

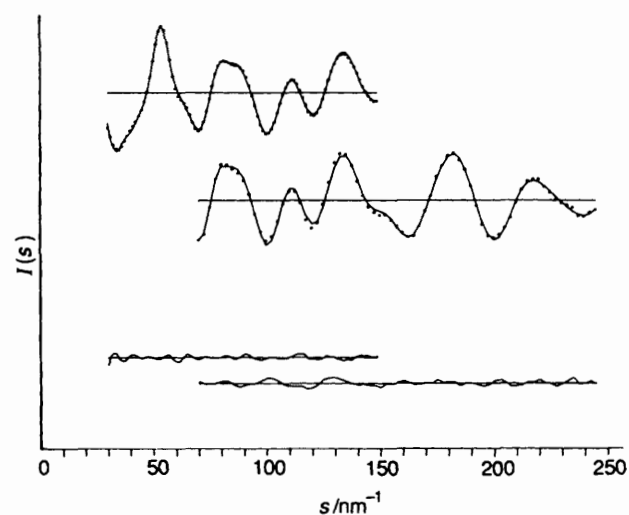


Fig. 2 Calculated (full line) and experimental (●) intensity curves for $\text{V}(\text{OBu}')_4$ with the difference curves shown below

Exploratory refinements with non-planar co-ordination of the nitrogen atoms did not improve the fit to the experimental data. A molecular model of $\text{Ti}(\text{NMe}_2)_4$ is shown in Fig. 3. This model is described by three bond distances, M–N, N–C and C–H, three bond angles, $\text{N}^*-\text{M}-\text{N}$ (see Fig. 3), M–N–C and N–C–H, and two dihedral angles $\varphi(\text{N}^*\text{MNC})$ and $\varphi(\text{MNCH})$. When $\varphi(\text{N}^*\text{MNC})$ is 0 (*i.e.* when the two NC_2 groups are coplanar) or 90° the molecular symmetry is D_{2d} .

The eight independent parameters and eight root-mean-square vibrational amplitudes were refined in a least-squares fit of a calculated to the experimental intensity curve. For both amides the absolute value of all correlation coefficients was less than 68%.

In their study of $\text{Zr}(\text{NMe}_2)_4$, which is pseudo-isoelectronic with $\text{Ti}(\text{NMe}_2)_4$, Rice and co-workers² found the gas-phase electron diffraction data to be equally compatible with a D_{2d} model with $\varphi(\text{N}^*\text{MNC}) = 0^\circ$ and an S_4 model with $\varphi(\text{N}^*\text{MNC}) = 66^\circ$. Initial refinements of $\text{Ti}(\text{NMe}_2)_4$ with $\varphi(\text{N}^*\text{MNC})$ fixed at 0 yielded an *R* factor of 0.111. When $\varphi(\text{N}^*\text{MNC})$ was refined it increased to $51(1)^\circ$ and the *R* factor decreased to 0.041. Refinements with starting values for $\varphi(\text{N}^*\text{MNC})$ spaced at 10° intervals between 0 and 90° all converged to this least-squares minimum. We conclude that a D_{2d} model of $\text{Ti}(\text{NMe}_2)_4$ is inconsistent with our data.

$\text{V}(\text{OBu}')_4$. In our study of $\text{Cr}(\text{OBu}')_4$ we investigated four

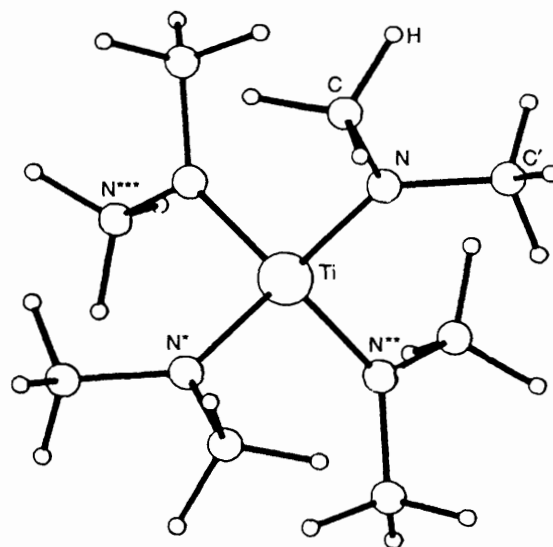


Fig. 3 Molecular model of $\text{Ti}(\text{NMe}_2)_4$ of S_4 symmetry viewed down the S_4 axis

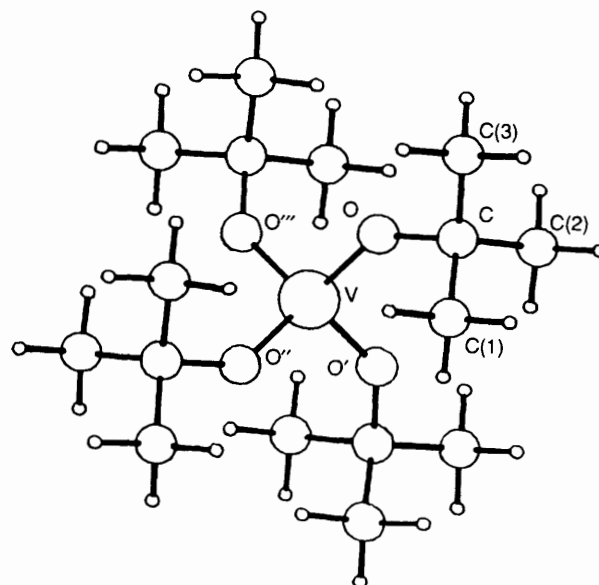


Fig. 4 Molecular model of $\text{V}(\text{OBu}')_4$ of S_4 symmetry viewed down the S_4 axis

models of D_{2d} , D_2 or S_4 symmetry.³ The only model which could be brought into satisfactory agreement with the data was an S_4 model similar to the one shown in Fig. 4. Since the radial distribution curves of the two molecules are indistinguishable we based our structure refinement of $\text{V}(\text{OBu}')_4$ on the same model. The $\text{C}(\text{CH}_3)_3$ and CCH_3 fragments were assumed to have local C_{3v} symmetry. The model is determined by four bond distances [$\text{V}-\text{O}$, $\text{O}-\text{C}$, $\text{C}-\text{C}$ (mean) and $\text{C}-\text{H}$], four valence angles ($\text{O}-\text{V}-\text{O}'$, $\text{V}-\text{O}-\text{C}$, $\text{O}-\text{C}-\text{C}$ and $\text{C}-\text{C}-\text{H}$), two dihedral angles, $\varphi(\text{O}'\text{VOC})$ and $\varphi(\text{VOCC})$, and a tilt angle. This tilt angle, *i.e.* the angle between the three-fold symmetry axis of the $\text{C}(\text{CH}_3)_3$ group and the $\text{O}-\text{C}$ bond, was defined as positive when the non-bonded $\text{V} \cdots \text{C}(1)$ and $\text{V} \cdots \text{C}(2)$ distances were increased. Refinements of the tilt angle failed to converge, and after some trial and error it was fixed at 0.6° which led to marginally better agreement than at 0° .

The remaining ten structure parameters and eleven vibrational amplitudes were refined in a least-squares fit of a calculated intensity curve to the experimental one. The correlation coefficients between the parameters $r(\text{O}-\text{C})$, $r(\text{C}-\text{C})$,

Table 2 Selected structure parameters, root-mean-square vibrational amplitudes (*l*) and *R* factors determined for the best model of Ti(NMe₂)₄ and V(NMe₂)₄. Estimated standard deviations in parentheses in units of the last digit. $R = [\sum w(I_{\text{obs}} - I_{\text{calc}})^2 / \sum w I_{\text{obs}}^2]^{1/2}$

	Ti(NMe ₂) ₄		V(NMe ₂) ₄	
	<i>r_a</i>	<i>l</i>	<i>r_a</i>	<i>l</i>
Bond distances/pm				
M-N	191.7(3)	5.9(3)	187.9(4)	5.8(4)
N-C	146.1(2)	4.0(3)	145.7(3)	5.1(4)
C-H	112.0(4)	6.9(4)	111.1(5)	7.4(5)
Bond angles/°				
M-N-C	124.3(3)		123.2(3)	
N-C-H	109.3(7)		112.5(9)	
N-M-N*	114.2(17)		100.6(5)	
N-M-N**	107.2(9)		114.1(1)	
Torsional angles/°				
φ(N*MNC)	51(1)		71(2)	
φ(MNCH)	20(2)		-28(2)	
Non-bonded distances/pm	<i>r_a</i>	<i>l</i>	<i>r_a</i>	<i>l</i>
M...C	299.4(4)	12.4(3)	294.1(3)	10.9(4)
N...N*	322(3)	22(3) ^a	289.2(10)	14(3) ^a
N...N**	309(2)	22(3) ^a	315.3(6)	14(3) ^a
N...H	211(1)	10.1(10)	214(1)	9.7(10)
C...C'	241.3(8)	8.1(10)	243.8(9)	7.6(13)
<i>R</i> factor of best model		0.041		0.049

^a Refined with equal shifts.**Table 3** Selected structure parameters, root-mean-square vibrational amplitudes (*l*) and *R* factors determined from the best model for V(OBu¹)₄. See Table 2 for definition of uncertainties and *R* factor

	<i>r_a</i>	<i>l</i>
Bond distances/pm		
V-O	177.9(6)	6.9(4)
O-C	143.3(15)	4.6(21)
C-C	152.7(7)	3.4(12)
C-H	110.4(4)	6.1(5)
Bond angles/°		
V-O-C	138.6(18)	
O-C-C	113.1(15)	
C-C-H	109.7(12)	
O-V-O'	115.1(19)	
O-V-O''	106.7(11)	
Torsional angles/°		
φ(O'VOC)	50(2)	
φ[VOCC(2)]	37(3)	
Non-bonded distances/pm	<i>r_a</i>	<i>l</i>
V...C	301(2)	7.5(11)
V...C(1)	340(2)	17.5(22)
V...C(2)	388(4)	51(20)
V...C(3)	417(1)	15.6(17)
C(1)...C(2)	243(3)	9.7(5) ^a
O...C(1)	248(2)	9.7(5) ^a
O...C(3)	246(2)	9.7(5) ^a
C...H	216(2)	10.0(13)
O...O'	300(3)	6.1(25) ^b
O...O''	285(2)	6.1(25) ^b
<i>R</i> factor of best model		0.055

^a Refined with equal shifts. ^b Refined with equal shifts.

l(O-C) and l(C-C) have absolute values in the range 74–91%. All other correlation coefficients are less than 66%.

All structure refinements were carried out with diagonal weight matrices. The formal estimated standard deviations calculated by the program, σ_{LS} , therefore include neither the uncertainty due to data correlation nor to non-refined parameters. The estimated standard deviations quoted in

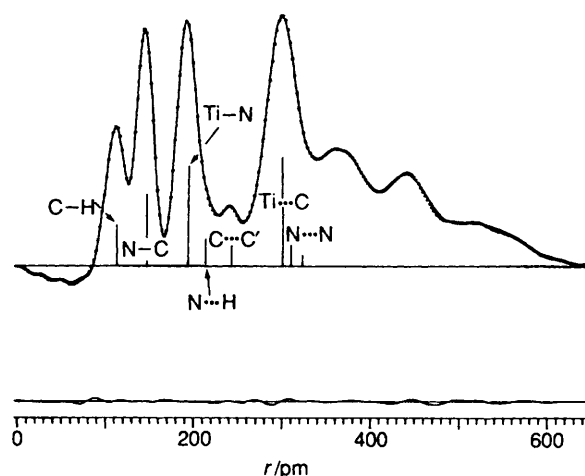


Fig. 5 Radial distribution curves for Ti(NMe₂)₄, experimental (●) and theoretical (full line). The artificial damping factor $k = 30 \text{ pm}^2$. The most important peaks are indicated by bars of height approximately proportional to the weight of the distance in the theoretical intensity curve. The difference curve is shown below

Tables 2 and 3 have been obtained from σ_{LS} by multiplication with a factor of three. They have also been expanded to include an estimated scale uncertainty of 0.1%.

Discussion

The parameters determined from the best model for the amides and the alkoxide are listed in Tables 2 and 3, respectively. The radial distribution curves for Ti(NMe₂)₄, V(NMe₂)₄ and V(OBu¹)₄ are shown in Figs. 5, 6 and 7, respectively.

No significant differences are found between the structures of the amide ligands in Ti(NMe₂)₄ and V(NMe₂)₄; in both compounds the co-ordination sphere of the N atom is trigonal planar.

Under the *S*₄ point group the four occupied *p_n* orbitals on the N atoms may be combined to form symmetry orbitals of A, B and E symmetry. The 3d orbitals on the metal atom transform like A, B (twice) and E. The two low-lying d orbitals in a

tetrahedral field, *viz.* $3d_{z^2}$ and $3d_{x^2-y^2}$, transform like A and B respectively. All p_x electrons on N may therefore be stabilized by

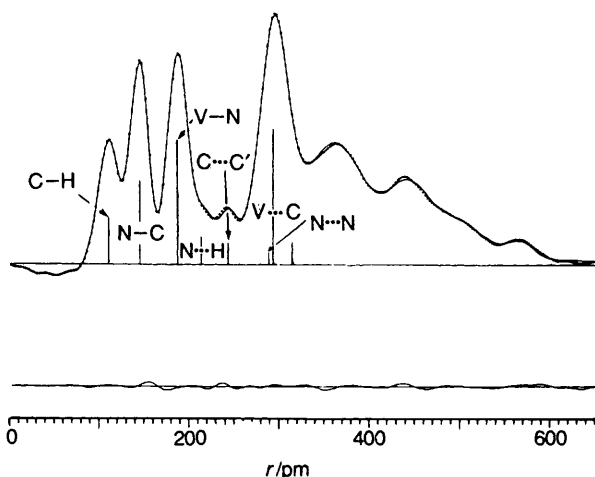


Fig. 6 Radial distribution curves for $V(NMe_2)_4$. Details as in Fig. 5

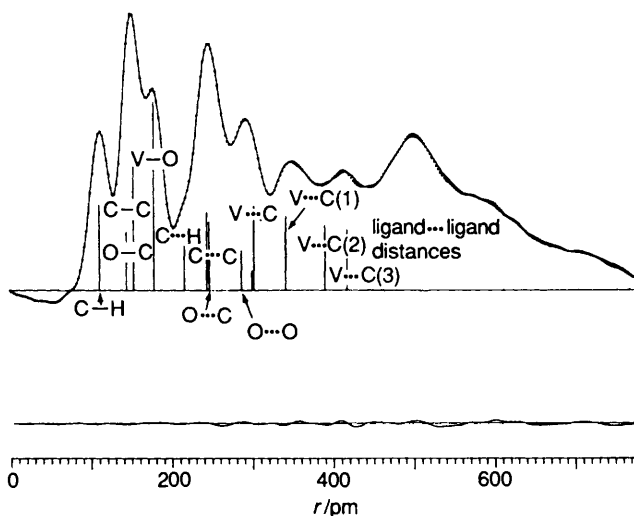


Fig. 7 Radial distribution curves for $V(OBu)_4$. Details as in Fig. 5

interactions with metal d orbitals, leading to partial π bonding between the N and metal atoms. The strongest interaction is however expected with the $3d_{z^2}$ and $3d_{x^2-y^2}$ orbitals.

Since the observed planar co-ordination of the N atoms may be due to repulsion between the methyl groups and the large metal atoms, we do not believe that this observation in itself is sufficient to establish that such π interactions are significant.

If the dihedral angle $\phi(N^*MNC)$ is 90° the non-bonding π -electron pairs on the N atoms interact only with the $3d_{z^2}$ orbital on the metal atom. If the dihedral angle is 0° they may interact with $3d_{x^2-y^2}$. The observed dihedral angle in the d^0 titanium amide, $51(1)^\circ$, is close to 45° , thus indicating that nitrogen π electrons are donated equally into both low-lying d orbitals. The N-Ti-N valence angle, $114(2)^\circ$, indicates that the co-ordination tetrahedron of Ti may be slightly flattened. The large value obtained for the N...N vibrational amplitudes, $22(3)$ pm, suggests, however, that the TiN_4 core undergoes relatively large-amplitude deformation vibrations.

In the d^1 vanadium amide the dihedral angle $\phi(N^*MNC)$ has increased to $71(2)^\circ$. This suggests that the additional electron on the metal atom occupies the $3d_{x^2-y^2}$ orbital and that the increased dihedral angle reflects a preference for donation of the nitrogen π electrons into the empty $3d_{z^2}$ orbital. Preferential donation of such electrons into the metal $3d_{z^2}$ orbitals would be expected to decrease the N^*-M-N angle, and N^*-V-N is indeed found to be significantly smaller than tetrahedral, $100.6(5)^\circ$. Measurements of spectroscopic and magnetic properties have led to the same conclusion.⁷

The structure of $Cr(NMe_2)_4$ is unknown, but that of $Mo(NMe_2)_4$ which is *diamagnetic* has been determined by X-ray crystallography.¹ The crystal contains two molecules in the asymmetric unit, both close to D_{2d} symmetry with $\phi(N^*MoNC) = 90^\circ$, indicating that the nitrogen π electrons are donated into the $4d_{z^2}$ orbital exclusively. The two d electrons presumably occupy the $4d_{x^2-y^2}$ orbital.¹ The N^*-M-N angles in crystalline $Mo(NMe_2)_4$ would consequently be expected to be smaller than tetrahedral. The N-Mo-N angles in the two crystallographically independent molecules are, however, found to vary in an apparently random manner between 107.3 and 112.5° ; it appears that in the crystalline phase the angles are determined by intermolecular forces.

The difference between the M-O bond distances in the *tert*-butoxides of V and Cr, $177.9(6)$ and $175.1(7)$ pm,³ is of the expected magnitude, but of marginal statistical significance. The O-M-O angle in the d^1 vanadium alkoxide is significantly greater than tetrahedral, corresponding to a flattened co-

Table 4 Observed metal-ligand bond distances (pm) in compounds MX_4 where M = Ti, V or Cr and WX_6 where X = alkyl, NMe_2 , alkoxy or F. Distances calculated from the metal bonding radii with those from the modified Schomaker-Stevenson rule^a in square brackets

M	X			
	CH_2CMe_3 $R(C) = 79^a$ $\chi(C) = 2.50^b$	NMe_2 $R(N) = 73^a$ $\chi(N) = 3.07^b$	$OCMe_3$ $R(O) = 72^a$ $\chi(O) = 3.50^b$	F $R(F) = 74^a$ $\chi(F) = 4.10^b$
Ti^{IV} $R = 137^c$ $\chi = 1.32^b$	—	$191.7(3)^d$ [191]	—	$175.4(3)^e$ [175]
V^{IV} $R = 130^c$ $\chi = 1.45^b$	—	$187.9(4)^d$ [186]	$177.9(6)^d$ [179]	—
Cr^{IV} $R = 128^c$ $\chi = 1.56^b$	$203.8(4)^f$ [199]	—	$175.1(7)^g$ [179]	$170.6(2)^h$ [171]
W^{VI} $R = 145^c$ $\chi = 1.40^b$	$214.6(3)^i$ [214]	$203.5(5)^j$ [201]	$190.2(3)^k$ [193]	$183.2(3)^l$ [185]

^a Ref. 15. ^b Ref. 16. ^c Adjusted value, this work. ^d This work. ^e Ref. 17. ^f Ref. 4. ^g Ref. 3. ^h Ref. 18. ⁱ Ref. 19. ^j Ref. 20. ^k Ref. 21. ^l Ref. 22.

ordination tetrahedron, indicating preferential donation of oxygen π electrons into the $3d_{x^2-y^2}$ orbital and that the unpaired d electron occupies the $3d_{z^2}$ orbital. The dihedral angle $\varphi(O'VOC) = 50(2)^\circ$, however, does not favour donation into either of the two orbitals. It is suggested that the dihedral angle is determined by steric repulsion between the very bulky ligands. The d^2 chromium alkoxide³ is paramagnetic with a magnetic moment corresponding to two unpaired electrons, $(3d_{z^2})^1(3d_{x^2-y^2})^1$, and as expected the $O'-Cr-O$ angle, $112(3)^\circ$, is not significantly greater than tetrahedral.

To what extent do the bond distances indicate that they are shortened by partial π bonding? We have found that in simple molecules single bond distances between the eighteen main-group elements in Groups 14–17 and H can be predicted with an average error of 3.2 pm from the modified Schomaker–Stevenson (MSS) rule [equation (1)], where R is the bonding

$$R(A-B) = R(A) + R(B) - c|\chi(A) - \chi(B)|^{1.4} \quad (1)$$

radius, χ is the Allred–Rochow electronegativity and the constant $c = 8.5$ pm.¹⁵ Since the bonding radii of N, O and F have been adjusted to reproduce single bond distances to atoms without low-lying acceptor orbitals, we believe them to be suitable for estimation of single σ bonds to transition metals. In Table 4 we compare experimental and calculated bond distances obtained after adjustment of the bonding radii of the transition-metal atoms: $R = 137, 130, 128$ and 145 pm for Ti^{IV} , V^{IV} , Cr^{IV} and W^{VI} , respectively. The average difference between calculated and observed bond distances is about 2 pm. Thus, although dative π bonding may influence the valence angles at the metal and the orientations of the ligands, its effect on $M-X$ bond distances is uncertain.

Acknowledgements

We are grateful to the Norwegian Research Council for Science and the Humanities and the VISTA Program of Statoil and the Norwegian Academy of Science and Letters for financial support.

References

- 1 M. H. Chisholm, F. A. Cotton and M. W. Extine, *Inorg. Chem.*, 1978, **17**, 1329.
- 2 K. Hagen, C. J. Holwill, D. A. Rice and J. D. Runnacles, *Inorg. Chem.*, 1988, **27**, 2032.
- 3 E. G. Thaler, K. Rypdal, A. Haaland and K. G. Caulton, *Inorg. Chem.*, 1989, **28**, 2431.
- 4 R. A. Andersen, A. Haaland, K. Rypdal and H. V. Volden, *Acta Chem. Scand.*, 1991, **45**, 955.
- 5 D. C. Bradley and M. H. Gitlitz, *J. Chem. Soc. A*, 1969, 980.
- 6 S. G. Gibbins, M. F. Lappert, J. B. Pedley and G. J. Sharp, *J. Chem. Soc., Dalton Trans.*, 1991, **45**, 955.
- 7 E. C. Alyea and D. C. Bradley, *J. Chem. Soc. A*, 1969, 2330.
- 8 H. L. Krauss and G. Munster, *Z. Anorg. Allg. Chem.*, 1967, **24**, 352.
- 9 D. C. Bradley and M. L. Mehtra, *Can. J. Chem.*, 1962, **40**, 1183.
- 10 R. A. Andersen, D. B. Beach and W. L. Jolly, *Inorg. Chem.*, 1985, **24**, 4741.
- 11 W. Zeil, J. Haase and L. Wegmann, *Instrumentenk.*, 1966, **74**, 84.
- 12 O. Bastiansen, R. Graber and L. Wegmann, *Balzers High Vacuum Rep.*, 1969, **25**, 1.
- 13 B. Andersen, H. M. Seip, T. G. Strand and R. Stølevik, *Acta Chem. Scand.*, 1969, **23**, 3224.
- 14 L. Schäfer, A. C. Yates and R. A. Bonham, *J. Chem. Phys.*, 1971, **55**, 3055; *International Tables for X-Ray Crystallography*, Kynoch Press, Birmingham, 1974, vol. 4.
- 15 R. Blom and A. Haaland, *J. Mol. Struct.*, 1985, **128**, 21.
- 16 A. L. Allred and E. G. Rochow, *J. Inorg. Nucl. Chem.*, 1958, **5**, 264.
- 17 G. V. Girichev, V. M. Petrov, N. I. Giricheva and K. S. Krasnov, *Z. t. Strukt. Khim.*, 1982, **23**, 45.
- 18 L. Hedberg, K. Hedberg, G. L. Gard and J. O. Udeaja, *Acta Chem. Scand., Ser. A*, 1988, **42**, 318.
- 19 A. Haaland, A. Hammel, K. Rypdal and H. V. Volden, *J. Am. Chem. Soc.*, 1990, **112**, 4547.
- 20 K. Hagen, C. J. Holwill, D. A. Rice and J. D. Runnacles, *Acta Chem. Scand., Ser. A*, 1988, **42**, 578.
- 21 A. Haaland, K. Rypdal, H. V. Volden, J. E. Jacob and J. Weidlein, *Acta Chem. Scand.*, 1989, **43**, 911.
- 22 H. M. Seip and R. Seip, *Acta Chem. Scand.*, 1966, **20**, 2698.

Received 4th July 1991; Paper 1/03370K